

# A FILTER BANK APPROACH FOR LED ILLUMINATION SENSING BASED ON FREQUENCY DIVISION MULTIPLEXING

Hongming Yang<sup>†\*</sup>, Jan W. M. Bergmans<sup>†\*</sup>, Tim C. W. Schenk<sup>\*</sup>

<sup>†</sup>Eindhoven University of Technology, 5600 MB Eindhoven, The Netherlands.

<sup>\*</sup>Philips Research Europe - Eindhoven, 5656 AE Eindhoven, The Netherlands.

Email: h.m.yang@tue.nl, j.w.m.bergmans@tue.nl, tim.schenk@philips.com

## ABSTRACT

In this work, we consider illumination sensing in a light emitting diode (LED) based illumination system that normally consists of a large number of LEDs. Illumination sensing is used in order to facilitate the control of such system whose complexity, due to the large number of LEDs, can be quite high. In this paper, key requirements, i.e. accuracy and speed, on illumination sensing are described. Furthermore, we present a filter bank sensor structure based on frequency division multiplexing. The design of the filter response is discussed in the context of supporting maximum number of LEDs, while the key requirements on illumination sensing are satisfied. In particular, it is shown that, through the use of the filter with a triangular filter response, a large number of LEDs can be supported in the presence of frequency offsets in a practical range.

**Index Terms**— Illumination Sensing, Filter Banks, Frequency Division Multiplexing, Nyquist-1 Functions

## 1. INTRODUCTION

Due to the rapid development of solid state lighting technologies, considerable research interest has been devoted to light emitting diode (LED) based illumination systems. The considered systems normally consist of a large number of spatially distributed LEDs, which can be used to provide localized and dynamic lighting effects. To this end, the output illumination level of each LED is flexible and can be configured easily such that a desired lighting effect can be achieved at the location of interest, called target location.

Due to the large number of light sources, however, the complexity of calibrating and controlling such system can be quite high. In order to facilitate the control of such a high complexity system and to achieve engaging lighting effects, it is essential to accurately estimate the illumination contribution of each individual LED at the target location. This process is named illumination sensing [1] and is the focus of this paper. Further, for the purpose of illumination sensing, a sensor is located at the target location.

It is known that the illumination signal from each LED at the target location typically consists of repeatedly transmitted illumination pulses, as illustrated in Fig. 1, for the purpose of dimming the light [2]. The amplitude of the pulse, denoted by  $a_{i,i}$ , is the illuminance due to the  $i$ th LED. The value of  $a_{i,i}$  is fixed and determined by the optical output power of each LED and the free-space optical channel attenuation [1]. The duty factor of the pulse, denoted by  $p_i$  for the  $i$ th LED, in contrast, can be changed easily by a central controller. Through the setting of  $p_i$ , the output illumination level for each LED can be controlled individually in order to achieve desired

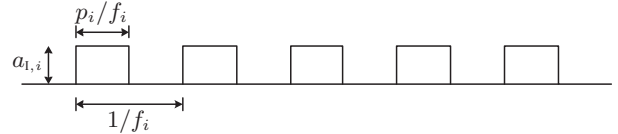


**Fig. 1.** Illumination pulse train due to the  $i$ th LED. The amplitude of the corresponding electrical pulse train equals  $a_i$ .

lighting effects at the target location. The illumination contribution of the  $i$ th LED is characterized by  $a_{i,i}p_i$ . Given the knowledge of each  $p_i$  at the central controller, it is thus sufficient to estimate  $a_{i,i}$  for each  $i$ . Furthermore, there are two key application requirements to the sensing process, viz. accuracy and speed, which will be elaborated in Section 2.

The illumination pulses from all LEDs simply sum up together at the target location. It is, however, difficult and expensive, if not impossible, to distinguish the signals from different LEDs optically. Instead, an electronic solution is desirable. Therefore, a photodiode is used to obtain an electrical pulse train. The electrical pulse train is of similar shape as that illustrated in Fig. 1, except that the amplitude is now the *electrical current*, denoted by  $a_i$  for the  $i$ th LED. Given that the conversion ratio  $a_i/a_{i,i}$  is known, we only need to estimate  $a_i$  for each  $i$ . To this end, one may adapt or shape the illumination waveform of Fig. 1 individually for each LED, in such a manner that the contributions can be disentangled electronically. For instance, the illumination pulses in Fig. 1 can be intermitted with deterministic pulse trains that serve as identifiers for the LEDs [1]. In such an approach, however, reliable recognition of the distinct identifiers requires complex procedures to maintain synchronism among the LEDs and between the LEDs and the sensor. In this paper, in contrast, we consider a much simpler asynchronous approach that is based on frequency division multiplexing (FDM). Here all LEDs are operated at different yet fixed  $f_i$  for the illumination pulse trains, with small yet easily discernible spacing, denoted by  $\Delta_f$ , between the different frequencies. The idea of setting the illumination pulse trains of the LEDs at distinct frequencies was proposed in [3]. The research challenges in this paper, however, are quite different from those in [3], since this paper focuses on a much higher number of LEDs and a much higher speed of illumination sensing.

The rest of the paper is organized as follows. Key system characteristics of the FDM approach and the key requirements on illumination sensing are presented in Section 2. Section 3 presents a filter bank sensor structure. Design of the filter bank is presented in Section 4. Performance evaluation is provided in Section 5. Finally, Section 6 concludes this paper.

## 2. SYSTEM CHARACTERISTICS

The electrical signal received at a sensor can be written as

$$y(t) = \sum_{i=1}^L y_i(t) + v(t) = \sum_{i=1}^L \sum_{n=-\infty}^{\infty} a_i h_i(t - t_i - \frac{n}{f_i}) + v(t), \quad (1)$$

where  $L$  is the number of LEDs,  $y_i(t)$  denotes the electrical signal due to the  $i$ th LED,  $v(t)$  is the noise, and the pulse shape  $h_i(t)$  is approximately rectangular with the exact shape determined by the on- and off-switch characteristics of the LEDs [1]. The duty cycle  $p_i$  of each pulse train is set on a logarithmic scale [4] and we have  $p_{\min} = 0.001 \leq p_i \leq p_{\max} = 0.97307$ . Here, we take the second largest value from [4] as  $p_{\max}$  since the FDM scheme cannot work at  $p_i = 1$ . Further, regarding the fundamental frequency, we have  $f_i \geq 75$  Hz in order to have no visible flicker from the LEDs. In order to maintain  $h_i(t)$  to be approximately rectangular for any  $p_i$ , we should also have  $\frac{p_{\min}}{f_i} \geq \tau_{\text{on}} + \tau_{\text{off}} \approx 250$  ns, where  $\tau_{\text{on}}$  and  $\tau_{\text{off}}$  denote the reaction time of the LEDs during on- and off-switch operations [2]. Hence we get  $f_i \leq 4$  kHz. Then we take the frequency range of  $f_i$  to be 2 kHz to 4 kHz, i.e. the bandwidth  $W = 2$  kHz, such that there is no possible overlap between  $f_i$  and the harmonics of any  $f_m$  where  $m \neq i$ . Moreover, frequency assignment is undertaken such that there is a uniform spacing  $\Delta_f$  between the neighboring frequencies, i.e.  $L = W/\Delta_f$ . The noise term  $v(t)$  in (1) is the sum of the electronics and shot noises. The double-sided power spectrum density of  $v(t)$  is denoted by  $N_0/2$ . For a practical indoor environment and a photodiode with an area of  $10 \text{ mm}^2$ ,  $N_0$  is typically in the order of  $10^{-24}$  ampere<sup>2</sup>/Hz. The value of  $a_i$  is, by contrast, in the order of  $10^{-6}$  ampere. Therefore, the noise is considered negligible in this paper. Finally, the term  $t_i$  denotes the initial phase shift of the signal and is unknown to the sensor. Now, we would like to estimate  $a_i$  for each  $i$  from  $y(t)$ . As introduced in Section 1, there are two key requirements:

1) Accuracy: It is known that the human visual system continuously adapts itself according to the background or environment lighting. Similarly, the *visibility* of an estimation error depends on the real illuminance level. Hence, in this paper, to gauge accuracy in illumination sensing, we normalize the estimation error with respect to the real illuminance. Since the illumination contribution of the  $i$ th LED is equivalently characterized by  $a_i p_i$ , we propose to characterize the requirement on the estimation of  $a_i$  by

$$\xi_i \triangleq 10 \log_{10} \left( |\hat{a}_i - a_i| p_i / (\sum_{m=1}^L a_m p_m) \right), \quad (2)$$

where  $\hat{a}_i$  denotes the estimated value for  $a_i$ . Further, from the experimental results in [5], we can conclude that, when  $\xi_i$  is less than  $-20$  dB, the estimation error is no longer visible to human eyes, irrespective of the circumstances.

2) Speed: We may consider the tolerance time between the moment when a user pushes a button and that when the illumination level of a lamp is changed and enters a stable state. Therefore, a *response time*, denoted by  $T$ , that is significantly below one second, is expected. More specifically, in this paper, we require  $T \leq 0.1$  s.

When the above two requirements are satisfied, it is desirable to be able to support as many LEDs as possible, since more LEDs will provide more degrees of freedom to create flexible lighting effects.

## 3. SENSOR SIGNAL PROCESSING

The main challenge for the sensor processing is to separate the signals from different LEDs and then to estimate each  $a_i$ . In the FDM

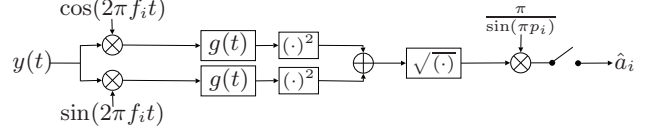


Fig. 2. Block diagram of the filter bank estimator.

scheme, the spectrum of  $y_i(t)$  can be obtained as

$$Y_i(f) = \sum_{n=-\infty}^{\infty} a_i f_i H_i(f) e^{-j2\pi f t_i} \delta(f - n f_i), \quad (3)$$

where  $\delta(\cdot)$  denotes the Kronecker delta function and  $H_i(f)$  is the Fourier transform of  $h_i(t)$ ,  $H_i(f) = \int_{-\infty}^{\infty} h_i(t) e^{-j2\pi f t} dt$ . Therefore,  $Y_i(f)$  consists of multiple lines at frequencies  $n f_i$  where  $n = 0, \pm 1, \pm 2, \dots$ . In this paper, we present an approach that is based only on the fundamental frequency components, i.e.  $n = \pm 1$ . The reasons for taking only  $n \pm 1$  are two-fold. First, each  $f_i$  is distinct while there is potential overlap in the higher harmonics of  $f_i$  for different  $i$ . Secondly, it is already sufficient to estimate each  $a_i$  from the fundamental frequency component alone by  $\hat{a}_i = \frac{|Y_i(f_i)|}{f_i H_i(f_i)} = \frac{\pi}{\sin(\pi p_i)} |Y_i(f_i)|$ , where the second equality is because  $h_i(t)$  is approximately a rectangular function with duty cycle  $p_i$ .

In order to separate the signals from different LEDs, we consider applying a bank of bandpass filters to  $y(t)$ , followed by an envelope detector. The filter response corresponding to the  $i$ th LED is denoted by  $G_i(f)$ . Due to the uniform frequency spacing  $\Delta_f$  between LEDs, it is sufficient to design the filters such that  $G_i(f) = G(f - f_i) + G^*(-f - f_i)$  where  $G(f)$  is a lowpass filter and is identical for every  $i$ . Further, we assume  $g(t)$ , which is the inverse Fourier transform of  $G(f)$ , is a real-valued function, and thus  $G^*(-f) = G(f)$ . Hence we have  $G_i(f) = G(f - f_i) + G(f + f_i)$  and equivalently  $g_i(t) = 2g(t) \cos(2\pi f_i t)$ . The envelope of the filtered signal  $y(t) * g_i(t)$ , where  $*$  denotes the convolution operation, can then be written as  $\left| \int_{t-T}^t 2y(\phi) e^{j2\pi f_i \phi} g(t - \phi) d\phi \right|$ . More specifically, the estimated value can be written as

$$\hat{a}_i = \hat{a}_i(t) = \frac{\pi}{\sin(\pi p_i)} \left| \int_{t-T}^t y(\phi) e^{j2\pi f_i \phi} g(t - \phi) d\phi \right|. \quad (4)$$

The block diagram of the filter bank is then given in Fig. 2. The support of  $g(t)$ , i.e. the time interval when  $g(t) \neq 0$ , determines the period of time for the filter to generate a stable output after a user enables a sensing operation. Therefore, the response time  $T$  of the sensing operation is mainly determined by the support of  $g(t)$ . In the following, we thus assume the support of  $g(t)$  is  $0 \leq t \leq T$ .

## 4. DESIGN OF THE FILTER RESPONSE

From (4), the performance of the illumination sensing is quite dependent on the design of  $G(f)$ . In this section, we hence consider the design of  $G(f)$ .

### 4.1. Ideal Case without Frequency Offsets

First, we assume there are no frequency inaccuracies in any  $f_i$ . From (1), (3) and (4), we get

$$\hat{a}_i = \left| a_i G(0) + \sum_{m \neq i} a_m \frac{\sin(\pi p_m)}{\sin(\pi p_i)} \frac{e^{j2\pi(m-i)\Delta_f t}}{e^{j2\pi(f_m t_m - f_i t_i)}} G((m-i)\Delta_f) \right|$$

where noise is neglected. Thus, the estimation error

$$|\hat{a}_i - a_i| \leq a_i |G(0) - 1| + \sum_{m \neq i} a_m \frac{\sin(\pi p_m)}{\sin(\pi p_i)} |G((m-i)\Delta_f)|.$$

Then, we can perfectly separate the signals from different LEDs, and thus the optimum estimation performance can be achieved, if the following conditions on  $G(f)$  are satisfied.

**Condition (a):**  $G(0) = 1$ .

**Condition (b):**  $G(n\Delta_f) = 0$  for  $n \neq 0$ .

**Condition (c):**  $g(t)$  is real-valued with support  $0 \leq t \leq T$ .

From the first two conditions, we obtain that  $G(f)$  is actually a Nyquist-1 function of  $f$ , satisfying the Nyquist pulse shaping criterion [6]. Therefore we have  $\sum_n g(t + n/\Delta_f) = \Delta_f$ . Thus the minimum support of  $g(t)$  is  $1/\Delta_f$ , which is achieved when and only when  $g(t)$  equals a rectangular function  $g(t) = \frac{1}{T} \text{rect}(\frac{t}{T} - \frac{1}{2})$ , where  $\text{rect}(t) = 1$  if  $|t| \leq 1/2$  and  $\text{rect}(t) = 0$  elsewhere. Hence, we have  $T \geq 1/\Delta_f$  and  $L = W/\Delta_f \leq WT$ , with the equality achieved only by setting  $g(t)$  to be rectangular. In other words, given the requirement on  $T$ , the rectangular function can support the largest number of LEDs by  $L_{\max} = WT$ .

## 4.2. In the Presence of Frequency Offsets

In practice, there is always some frequency inaccuracy in  $f_i$ . The frequency offset equals  $\epsilon_i \triangleq f_i - \bar{f}_i$  (in Hz), where  $f_i$  and  $\bar{f}_i$  denote the actual and ideal fundamental frequency, respectively. The estimation error can thus be obtained similarly to Section 4.1. Specifically, without loss of generality, we focus on the estimation of  $a_1$ , the cost function (2) can be written as  $\xi_1 \leq 10 \log_{10}(\xi_1^b + \xi_1^i)$ , and

$$\xi_1^b = \left[ 1 + \frac{\sum_{m=2}^L a_m p_m}{a_1 p_1} \right]^{-1} (1 - |G(\epsilon_1)|),$$

$$\xi_1^i = \frac{1}{\pi \text{sinc}(\pi p_1)} \frac{\sum_{m=2}^L a_m \sin(\pi p_m) |G((m-1)\Delta_f + \epsilon_m)|}{\sum_{m=1}^L a_m p_m}$$

which are named *bias error* and *interference*, respectively. Through the first-order Taylor expansion, we get

$$G(\epsilon_1) = 1 + G'(0)\epsilon_1 + O(\epsilon_1^2),$$

$$G((m-1)\Delta_f + \epsilon_m) = G'((m-1)\Delta_f)\epsilon_m + O(\epsilon_m^2),$$

where  $G'(f)$  denotes the derivative of  $G(f)$ . Therefore, in order to achieve an estimation performance that is robust against frequency offsets, we can design  $G(f)$  to be a Nyquist-1 function with an additional constraint

**Condition (d):**  $|G'(n\Delta_f)| = 0$ , for any integer  $n$ .

In order to obtain such functions, we first write  $G(f)$  as  $G(f) = G_1(f)G_2(f)$ , where  $G_1(f)$  is a Nyquist-1 function, which in general does not satisfy *Condition (d)*, and  $G_2(f)$  is an arbitrary function that is differentiable at  $n\Delta_f$ . Then

$$G'(n\Delta_f) = G_1(n\Delta_f)G_2'(n\Delta_f) + G_1'(n\Delta_f)G_2(n\Delta_f)$$

$$= G_1'(n\Delta_f)G_2(n\Delta_f), \quad \text{for } n \neq 0. \quad (5)$$

Thus *Condition (d)* is satisfied for  $n \neq 0$  if and only if  $G_2(n\Delta_f) = 0$ . Further,  $G_2(0) = 1$ , otherwise  $G(f)$  is no longer a Nyquist-1 function. Hence,  $G_2(f)$  is also a Nyquist-1 function. From Section 4.1, the minimum support is  $1/\Delta_f$  for both  $g_1(t)$  and  $g_2(t)$ , which are inverse Fourier transform of  $G_1(f)$  and  $G_2(f)$ , respectively. The minimal support of  $g(t)$  is thus  $2/\Delta_f$ , which is achieved when both  $g_1(t)$  and  $g_2(t)$  are rectangular functions, i.e.  $g(t)$  is a

triangular function. More specifically,  $g(t) = \frac{2}{T} \text{rect}(\frac{2t}{T} - \frac{1}{2}) * \frac{2}{T} \text{rect}(\frac{2t}{T} - \frac{1}{2})$ . It can be confirmed that this  $g(t)$  also satisfies  $G'(0) = 0$ . Hence, *Condition (d)* is satisfied at any  $n$ . Therefore, we have  $\frac{2}{\Delta_f} \leq T$  or  $L \leq \frac{1}{2}WT$ , where equality is achieved only by setting  $g(t)$  to be the triangular function.

Note that the design of Nyquist-1 functions with a similar requirement was also investigated in other application contexts and under different optimization criteria [7–9]. To our best knowledge, we are the first to give the constraint condition in the form of *Condition (d)* and to show that the triangular function has the minimum support, which is a desirable property for our application context.

We can of course further extend  $G(f)$  to be the product of three or more Nyquist-1 functions, which allows a higher clock inaccuracy. In this paper, however, since we focus on a practical case of 100 ppm (parts per million) clock inaccuracy, the triangular function already suffices, as will be shown in Section 5.

## 5. PERFORMANCE EVALUATION

In this section, we evaluate the performance of the presented filter bank estimator, in terms of sensing accuracy and the number of LEDs that can be supported. Here, we consider the case with 100 ppm clock inaccuracy for which  $|\epsilon_i| \leq 0.4$  Hz. Then, in order to make sure that the requirement on  $\xi_1 \leq -20$  dB is satisfied in all cases irrespective of  $\{a_m\}$ ,  $\{p_m\}$  and  $\{\epsilon_m\}$ , we consider the worst case conditions as follows.

From Section 4.2, we get  $10 \log_{10} \xi_1^b \leq 10 \log_{10} (1 - |G(\epsilon_1)|)$ , which can be evaluated to be well below  $-20$  dB for  $T \leq 0.1$  s. Therefore, we can neglect  $\xi_1^b$  and focus on the term  $\xi_1^i$ . Further, it is in principle easier to suppress the frequency components which are further apart from  $f_1$ . Therefore,

$$\xi_1^i \leq \max_{\epsilon_2} \frac{|G(\Delta_f + \epsilon_2)|}{\text{sinc}(\pi p_1)} \frac{\sum_{m=2}^L a_m \sin(\pi p_m)}{\sum_{m=2}^L a_m \pi p_m}$$

$$\leq \max_{\epsilon_2} \frac{\text{sinc}(\pi p_{\min})}{\text{sinc}(\pi p_{\max})} |G(\Delta_f + \epsilon_2)|, \quad (6)$$

because  $\text{sinc}(\pi p_1) \geq \text{sinc}(\pi p_{\max})$  and  $\frac{\sin(\pi p_m)}{\pi p_m} \leq \text{sinc}(\pi p_{\min})$  for each  $m$ . We thus have the worst case performance as

$$\xi_1 = 15.6 + 10 \log_{10} \max_{\epsilon_2 = \pm 0.4} |G(\Delta_f + \epsilon_2)|. \quad (7)$$

In particular, for the triangular function,

$$\xi_1 = 15.6 + 10 \log_{10} \max_{|\epsilon_2| = \pm 0.4} |\text{sinc}^2(\frac{1}{2}T\pi(\Delta_f + \epsilon_2))|. \quad (8)$$

Here, we only consider  $\epsilon_2 = \pm 0.4$ , i.e. the worst case with respect to  $\epsilon_2$ . We can evaluate the performance of the rectangular and triangular function as shown in Fig. 3. It can be seen that, at  $\Delta_f = 20$  Hz, there is significant improvement of the estimation performance in terms of  $\xi_1$ , compared to the use of the rectangular function.

Further, from (8), we can obtain the tradeoff between  $L$  and clock inaccuracy at given  $T$  as follows. At a very small clock inaccuracy, we know that  $L = \frac{1}{2}WT$  LEDs can be supported. Then, with a larger clock inaccuracy, i.e. a larger range of  $\epsilon_2$  in (8), the estimation error in terms of  $\xi_1$  will also increase. There is a boundary value for the clock inaccuracy when the requirement  $\xi_1 \leq -20$  dB will no longer be satisfied. Therefore, if the practical clock inaccuracy is larger than the boundary value, we have to reduce  $T$  proportionally such that  $T \cdot \max_{\epsilon_2} |\epsilon_2|$  does not increase. Thus,  $\Delta_f = \frac{2}{T}$  has to be in turn increased. Equivalently,  $L = \frac{W}{\Delta_f} = \frac{1}{2}WT$  is decreased.

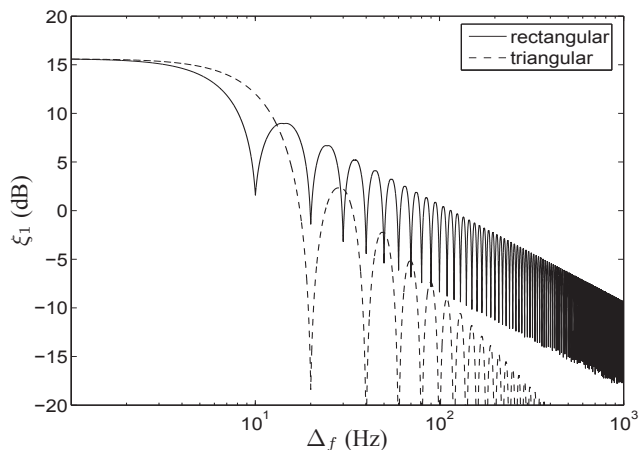


**Fig. 3.** The worst case  $\xi_1$  with respect to the frequency spacing, at  $T = 0.1$  s and 100 ppm clock inaccuracy.

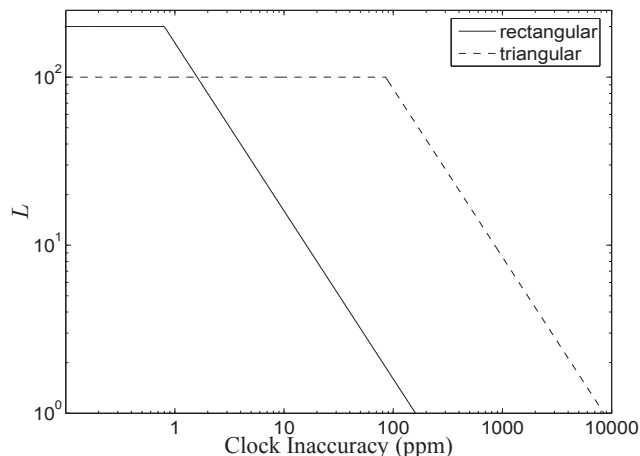


**Fig. 4.** The tradeoff between  $L$  and clock inaccuracy with  $T \leq 0.1$ .

The boundary value for the clock inaccuracy can be obtained through numerical evaluations. For instance, we can find that the boundary value is 85 ppm to satisfy  $\xi_1 \leq -20$  dB and  $T \leq 0.1$  second. Therefore, we can obtain the tradeoff between the clock inaccuracy and  $L$ , as shown in Fig. 4. From Fig. 4, we can also conclude that we can support at maximum  $L = 85$  LEDs at 100 ppm clock inaccuracy.

Moreover, the requirement on  $T$  might be relaxed in certain practical application scenarios. Therefore, it is of high practical value to investigate the tradeoff between  $L$  and  $T$  at 100 ppm clock inaccuracy, provided that the condition on  $\xi_i \leq -20$  dB is always satisfied. We know that, when  $T$  increases from zero,  $L$  is linearly proportional to  $T$  by  $L = \frac{1}{2}WT$ . However, the increase of  $T$  will result in a higher  $\xi_1$  at given clock inaccuracy from (8). When  $T$  spans beyond  $T_{\max} = 0.085$  s, the requirement on  $\xi_1 \leq -20$  dB will no longer be satisfied. Thus in practice, we would maintain  $T = 0.085$  s even if we are allowed to have a larger  $T$ . The tradeoff between  $T$  and  $L$  for the triangular function at 100 ppm can thus be obtained as depicted in Fig. 5. The tradeoff between  $T$  and  $L$  for different clock inaccuracies can also be obtained similarly. From Fig. 5, in order to accommodate more LEDs, we need to both increase  $T$  and reduce the clock inaccuracy.

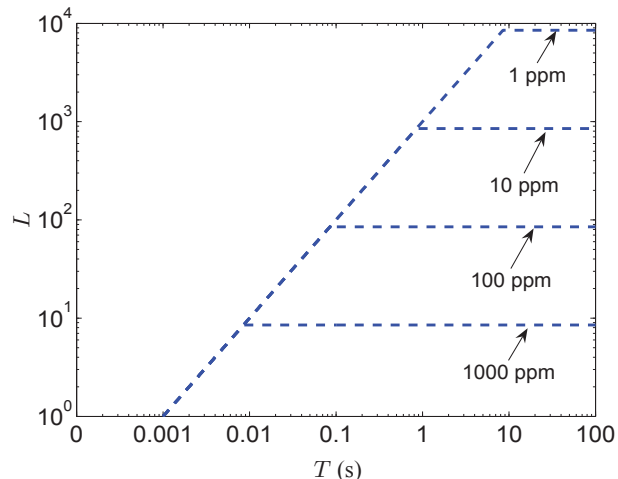


**Fig. 5.** The number of LEDs  $L$  vs. response time  $T$  for the triangular function at different clock inaccuracies.

## 6. CONCLUSION

In this paper, a filter bank sensor structure is presented for the purpose of illumination sensing based on FDM in LED lighting systems. The design of filter responses, in the context of supporting maximum number of LEDs while satisfying the estimation requirements on high speed and accurate illumination sensing, is also discussed. We showed that a large number of LEDs can already be accommodated with a simple FDM scheme and a filter-bank based sensor structure, through the use of the triangular function as the filter response. We also note that the filter with a triangular impulse response can be implemented at a very low cost by applying the concatenation of two sliding window integrators.

## 7. REFERENCES

- [1] J.-P. M. G. Linnartz, et al., "Communications and sensing of illumination contributions in a power LED lighting system," in *IEEE Proc. ICC*, May. 2008, pp. 5396–5400.
- [2] Luxeon STAR LEDs. [Online]. Available: <http://www.luxeonstar.com/faqs.php>
- [3] M. Salsbury and I. Ashdown, "Adapting radio technology to LED feedback systems," *Proceedings of SPIE*, vol. 6669, 2007.
- [4] IEC 62386, "Digital addressable lighting interfaces," 2007.
- [5] P. R. Boyce, *Human Factors in Lighting, Second Edition*. CRC, 2003, ch. 2.
- [6] J. G. Proakis, *Digital Communications*. McGraw Hill, 2000, ch. 9.
- [7] L. E. Franks, "Further results on Nyquist's problem in pulse transmission," *IEEE Trans. Commun. Technol.*, vol. 16, pp. 337–340, 1968.
- [8] J. Q. Scanlan, "Pulses satisfying the Nyquist criterion," *Electron. Letter*, vol. 28, pp. 50–52, 1992.
- [9] N. C. Beaulieu and M. O. Damen, "Parametric construction of Nyquist-I pulses," *IEEE Trans. Commun.*, vol. 52, pp. 2134–2142, 2004.